PHOTOCHEMICAL ELECTROCYCLIZATION OF THE ALLYL RADICAL INTO THE CYCLOPROPYL RADICAL

K. HOLTZHAUER, C. COMETTA-MORINI AND J. F. M. OTH*

Laboratory of Organic Chemistry, Swiss Federal Institute of Technology, ETH-Zentrum, CH-8092 Zürich, Switzerland

Following the observation that allyl radicals trapped in an argon matrix can be photolytically converted into cyclopropyl radicals ($\lambda = 410$ nm, 18 K), the IR spectrum of the cyclopropyl radical was recorded for the first time and interpreted. Bicyclopropane and cyclopropane are formed when the photolysed argon matrix is warmed from 18 to 35 K. The identification of these new species unequivocally proves the presence of cyclopropyl radicals in the photolysed matrix. This radical is shown to be a σ-type (C_s symmetry) and not a π-type (C_{2v} symmetry) radical; of the 18 normal frequencies of the C_s cyclopropyl radical, all active in the IR, 16 were observed and were assigned to their corresponding normal modes. For this assignment advantage was taken of *ab initio* frequency computations reported in the literature and performed by the authors.

INTRODUCTION

The thermal ring opening of the cyclopropyl radical to the allyl radical,[1-5] although symmetry forbidden in the ground state,[6,7] proceeds very easily because ring strain is released along the reaction pathway. This reaction should be strongly exothermic; in fact, *ab initio* calculations (see below) indicate that the allyl radical is ca 33 kcal mol^{-1} more stable than the cyclopropyl radical.

The cyclopropyl radical should therefore be very difficult to obtain and can be expected to be identified only as a transient species in selected reactions or as an isolated species eventually trapped in a rare gas matrix. The ESR spectrum of a species attributed to be cyclopropyl radical has been detected in the presence of many other paramagnetic species by Fessenden and Schuler[8] in liquid cyclopropane irradiated at $-120\,°C$ by a 2.8-MeV electron beam from a Van der Graff accelerator. Dupuis and Pacansky[9] unsuccessfully tried to trap the cyclopropyl radical in an argon matrix generated by photolysis and pyrolysis (at 600 °C) of acetylcycloproplyl peroxide. Dyke *et al.*[10] obtained the PE spectrum of the postulated cyclopropyl radical by reacting cyclopropane with fluorine atoms in the gas phase.

In the course of our studies on the allyl radical trapped in rare gas matrices,[11] we have observed that the allyl radical, when irradiated at 410 nm, i.e. in the first absorption band, undergoes ring closure yielding the cyclopropyl radical. Following this observation, we have investigated this photochemical reaction more extensively; this allowed us to record the first IR spectrum of the cyclopropyl radical trapped in an argon matrix (18 K) and, in independent experiments, to obtain some information about its ESR and its UV absorption spectra.

EXPERIMENTAL

Matrix preparation and instrumentation. The allyl radical, generated by flash vacuum pyrolysis at 850 °C of hexa-1,5-diene, was trapped with argon (Matheson, research purity) on a CsI crystal maintained at 18 K.

Our cryogenic equipment[12] consists of a laboratory-made liquid helium cryostat with CsI windows that can be slid in and out the beam of an IR spectrometer (Perkin-Elmer 983). The inner part of the cryostat, composed of a liquid helium reservoir, a temperature-controlled liquid helium vaporization chamber and a gold-plated copper block fitted with a CsI crystal (10 mm thick), is turnable around its vertical axis. A metal shutter, activated via a rotatory motion feed-through, is used to protect the CsI windows during the matrix deposition; it opens to either the spectrometer or the pyrolysis oven. The desired deposition temperature is adjusted and controlled ($\pm 0\cdot05$ K) via an electrical winding located around the liquid helium vaporization chamber, the temperature being sensed by a calibrated silicon diode (Lake Shore Cryotronics); the temperature

* Author for correspondence.

of the CsI crystal is measured (to ±0.02 K) via another calibrated silicon diode.

The pyrolysis oven, consisting of a quartz tube fitted in a Monel-600 cylinder heated by a thermocoax winding, is focused on the CsI crystal. The temperature of the oven is measured and controlled by a thermocouple (type K). At the oven inlet, three inclined holes divert the molecular beam (substance to be pyrolysed + rare gas) so that the molecules hit the inner wall of the quartz tube several times. In addition, rare gas at room temperature is sprayed directly on to the cold CsI crystal by six nozzles.

The necessary vacuum, typically in the region of 10^{-7} mbar (10^{-6} mbar during the matrix deposition), is generated by a turbomolecular pump (Pfeifer TPU 170) backed by a double-stage rotary pump (Pfeifer DUO 004). A more detailed description of the equipment will be published elsewhere.[12]

A general procedure for the matrix preparation was the following: hexadiene gas (10 mbar, 1 l) was diluted in argon (500 mbar, 1 l) and the gas mixture was introduced into the oven through a needle valve (Whitey SS-21-RS-2) at a rate of about 2 mmol h^{-1} for about 3 h (flow-rate calculated from the pressure drop of the gas mixture contained in a 1-l reservoir). At the same time, additional argon (14·5 mmol h^{-1}) was sprayed directly on to the CsI crystal. Under these conditions, a final matrix/host ratio of about 500 : 1 was obtained.

The IR spectrum of the matrix was then recorded with a PE-983 IR spectrophotometer equipped with a PE-3600 data station. The scan conditions were selected (mode 7, noise filter 4) in order to achieve a resolution of 0·5–1 cm^{-1} and a good signal to noise ratio. The spectra were stored on floppy disk for further transformation.

The cryostat was then slid away from the IR beam into the photolysis equipment. This installation consists of a water-cooled 1000-W super-pressure mercury lamp (Philips SP 1000 W) a Bausch and Lomb low-dispersion monochromator (gratings: 1200 grooves mm^{-1}) and appropriate optics to focus the exit slit (3 × 10 mm) of the monochromator on the matrix (magnification: 1 ×). The entrance and exit slits of the monochromator were chosen in order to obtain a spectral band width of ca 20 nm. The light power density at the wavelength selected for the irradiation experiments (410 nm) and at the position of the CsI crystal was measured with a power meter (Newport Powermeter Model 815) and found to be of 12 mW cm^{-2} (i.e. 10^{15} photons s^{-1} cm^{-2}). The IR spectrum of the irradiated matrix was recorded after several irradiation time intervals in order to determine the irradiation time giving the highest possible concentration of photoproducts. The maximum concentration of cyclopropyl radicals was obtained after ca 6–7 h of irradiation. The IR spectrum was then recorded after different warming and cooling cycles, this procedure being used for the assignment of the IR bands to the relevant chemical species formed.

RESULTS AND INTERPRETATION

The IR spectrum of the pyrolysis products of the allyl precursor hexa-1,5-diene is shown in Figure 1a. The assignment of the IR bands of this spectrum to the relevant chemical species trapped is given in Table 1. The bands assigned to the allyl radical are indicated by arrows in the spectrum. Their assignment to the allyl radical is based on their thermal behaviour and on *ab initio* calculations; a full vibration analysis (including isotope labelling measurements) was also performed and will be published elsewhere.[11]

When the 18 K argon matrix containing allyl radicals is irradiated at 410 nm, i.e. in the first absorption band ($^2A_2 \rightarrow \,^2B_1$) of allyl, the IR bands assigned to the allyl radical decrease in intensity and new bands appear. Figure 1b shows the IR spectrum obtained after 6·5 h of irradiation. These new bands can be more clearly seen in the difference spectrum (spectrum in Figure 1a minus that in Figure 1b, properly scaled) in Figure 2. Some of these bands have been assigned to the cyclopropyl radical.

This assignment, indicated in Table 2, is based on a comparison with the spectrum recorded after warming the matrix to 37 K and recooling it to 28 K (Figure 1c); this temperature rise leads to the formation of bicyclopropyl (dimerization of cyclopropyl radical) and also cyclopropane, thus proving the presence of the cyclopropyl radical before the matrix warm-up. Table 3 reports the assignment of the different new bands appearing on thermal treatment of the irradiated matrix (spectrum in Figure 1c). The IR absorptions assigned to bicyclopropyl and to cyclopropane were identified by independent measurements of the pure substances trapped in the argon matrix. The IR spectra of these reference substances are shown in Figures 3 and 4 and the bands positions observed are reported in Tables 4 and 5, together with indications of their thermal behaviour.

It should be noted that on warming the irradiated matrix to 37 K, cyclopropane is obviously formed by the cyclopropyl radical abstracting an H atom from hexa-1,5-diene present in the matrix; this is to be expected in view of the difference in the bond dissociation energies of a CH bond in cyclopropane and a CH bond in the allylic position in hexadiene. In fact, some IR bands in Figure 1c can be assigned unambiguously to the expected hexadienyl radical; for instance, the intense bands at 968 and 784 cm^{-1} are assigned to the CH out-of-plane vibration and CH$_2$ wagging in the allylic residue of the hexadienyl radical, respectively [the corresponding frequencies in allyl appear at 984/975 cm^{-1} (γCH) and 802 cm^{-1} (ωCH$_2$); see Tables 1–3].

Scheme 1 summarizes the different chemical and photochemical steps implied in the above-reported experiments.

It should be mentioned that, in different attempts to improve the yield of cyclopropyl radicals by photolysis, we observed that both cyclopropane and bicyclopropyl
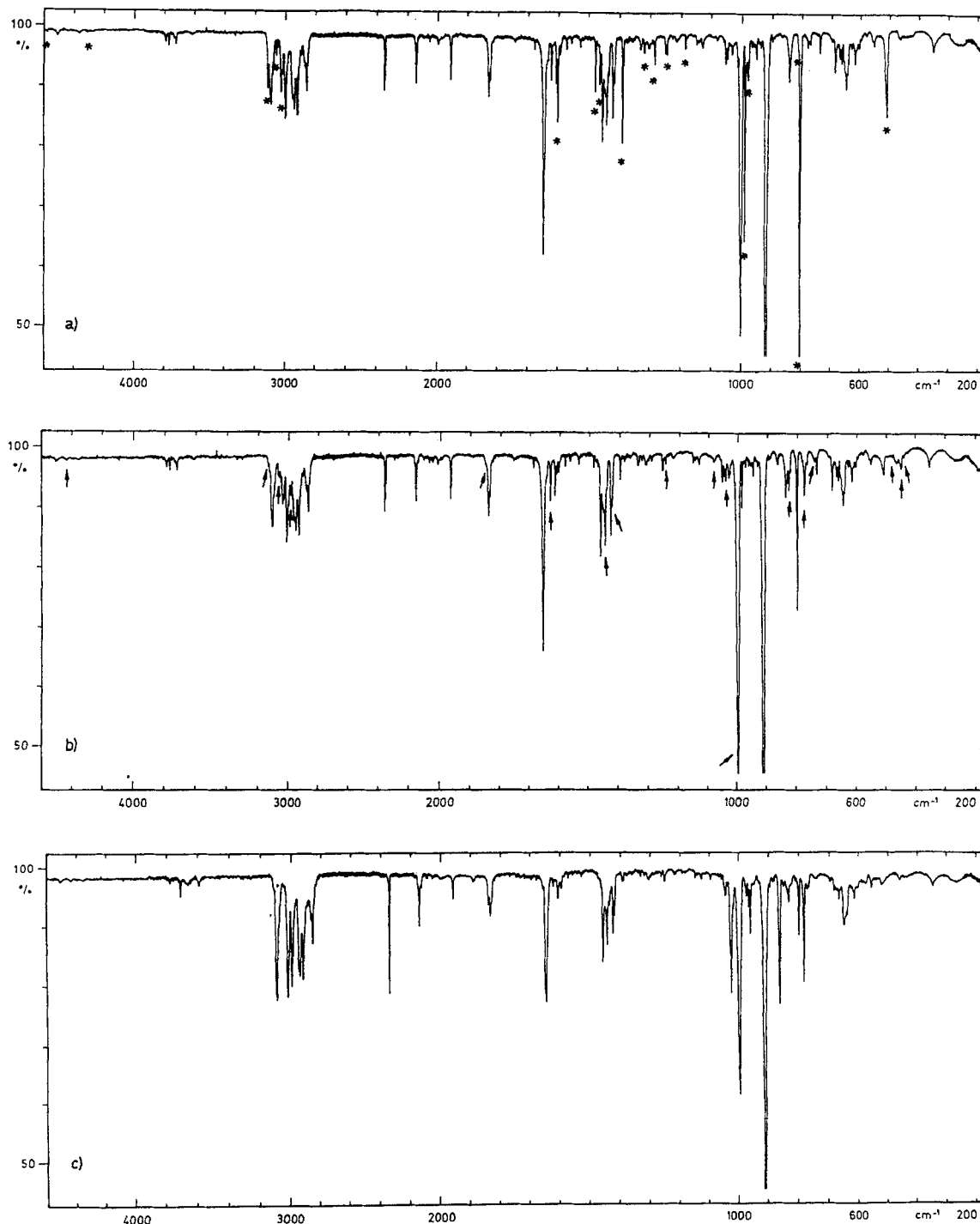
Figure 1. IR spectra of pyrolysis products (850 °C) of hexa-1,5-diene in an argon matrix (4·6 μmol cm⁻² hexadine, matrix/host ratio = 550 : 1). (a) Before irradiation at 18 K; asterisks indicate allyl radical; (b) after irradiation (λ = 410 nm) at 18 K; arrows indicate cyclopropyl radical; (c) after warming up to 37 K; spectrum recorded at 28 K

Table 1. Assignment of the different IR absorptions observed in the spectrum in
Figure 1a[a,b]

$$CH_2=CHCH_2CH_2CH=CH_2 \xrightarrow[850\,^\circ C]{\Delta} 2CH_2\dot{=}\dot{C}H\dot{=}CH_2$$

ν (cm^{-1})		Assignment	ν (cm^{-1})		Assignment	ν (cm^{-1})		Assignment
4560	vw	a.r.	1827	m	h	1043	w	h
4495	w	h	1680	w	all	1028	w	h
4345	vw	h	1650	s	h	1009	m	h
4290	vw	a.r.	1624	w	H$_2$O	997	vs	h
3775	vw	H$_2$O	1608	w	H$_2$O	984	s	a.r.
3757	vw	H$_2$O	1604	m	a.r.	974	m	a.r.
3712	w	H$_2$O	1574	w	?	963	w	h
3320	vw	a.r.	1478	m	a.r.	954	w	h
3109	m	a.r.	1464	m	a.r.	947	w	Ethen?
3087	m	h	1455	s	h	914	vs	h
3077	w	h	1449	m	h	837	m	all
3051	w	a.r.	1445	m	h	810	sh	a.r.
3040	w	a.r.	1441	s	h	802	vs	a.r.
3019	m	a + h	1435	m	h	776	w	h
3012	m	h	1421	s	h	767	w	h
2993	m	h	1416	m	h	737	w	Ethin?
2947	m	h	1389	s	a.r. + all	684	m	h
2936	m	h	1330	w	h	670	m	h
2915	m	h	1317	w	a.r. + h	647	m	h
2889	v	h	1304	w	h	629	w	?
2861	w	h	1284	w	a.r.	619	m	h
2850	m	h	1248	w	h	604	w	h
2344	w	CO$_2$	1242	w	a.r.	558	w	h
2339	w	CO$_2$	1210	w	h	553	w	h
2142	w	CO	1183	w	a.r.	511	m	a.r.
2137	m	CO	1145	w	h	473	w	h
1999	w	h	1126	w	h	425	vw	?
1956	m	all	1076	vw	h	357	w	h + all
1831	m	h	1050	m	h	301	w	h

[a] a.r., Allyl radical; h, hexadiene; all, allene; ?, unknown.

[b] w, Weak; vw, very weak; m, medium; s, strong; vs, very strong; sh, shoulder.

were already formed when we photolysed allyl (hexa-1,5-diene is always present) in neon at 4 K or in argon at 28 K (matrix/host ratio = 600). Evidently, the cyclopropyl radicals formed can diffuse at these matrix temperatures and composition conditions.

AB INITIO COMPUTATIONS

The identified IR absorptions of allyl (Table 1) and of cyclopropyl (Table 2) radicals were assigned to their normal modes by comparison with ab initio calculated frequencies.[14] The assignment of the allyl bands is in complete accord with the full vibrational analysis reported elsewhere.[11] We also refer to the ab initio computations reported by Takada and Dupuis[13] (allyl radical) and Dupuis and Pacansky[9] (cyclopropyl radical).

Geometry optimization and energy determination

The geometries of allyl (C_{2v}) and cyclopropyl radicals

(C_s and C_{2v}) were optimized using the standard program GAUSSIAN82[15] and the split valence basis sets with polarization functions 6-31G*,[16] 6-31G**[17] and D95**.[18] The inclusion of electron correlation was considered by applying the Møller–Plesset[19] perturbation method using the 6-31G* basis set. The optimized geometries obtained are presented in Tables 6–8. The computed total energies (in atomic units) are reported in Table 9, from which it can be seen that the allyl radical is the most stable of the three radicals. It is 33.0–33.7 kcal mol^{-1} more stable than the cyclopropyl radical with C_s symmetry (σ-radical); this σ-type cyclopropyl radical is itself 3.9 kcal mol^{-1} more stable than the cyclopropyl radical with C_{2v} symmetry (π-radical). This value of 3·9 kcal mol^{-1} in fact represents the expected energy barrier of inversion at the radical centre of the cyclopropyl σ-type radical. That the π-radical is indeed the transition-state structure for this inversion is indicated by the fact that the CH bending vibration in the π-radical is found to be imaginary in
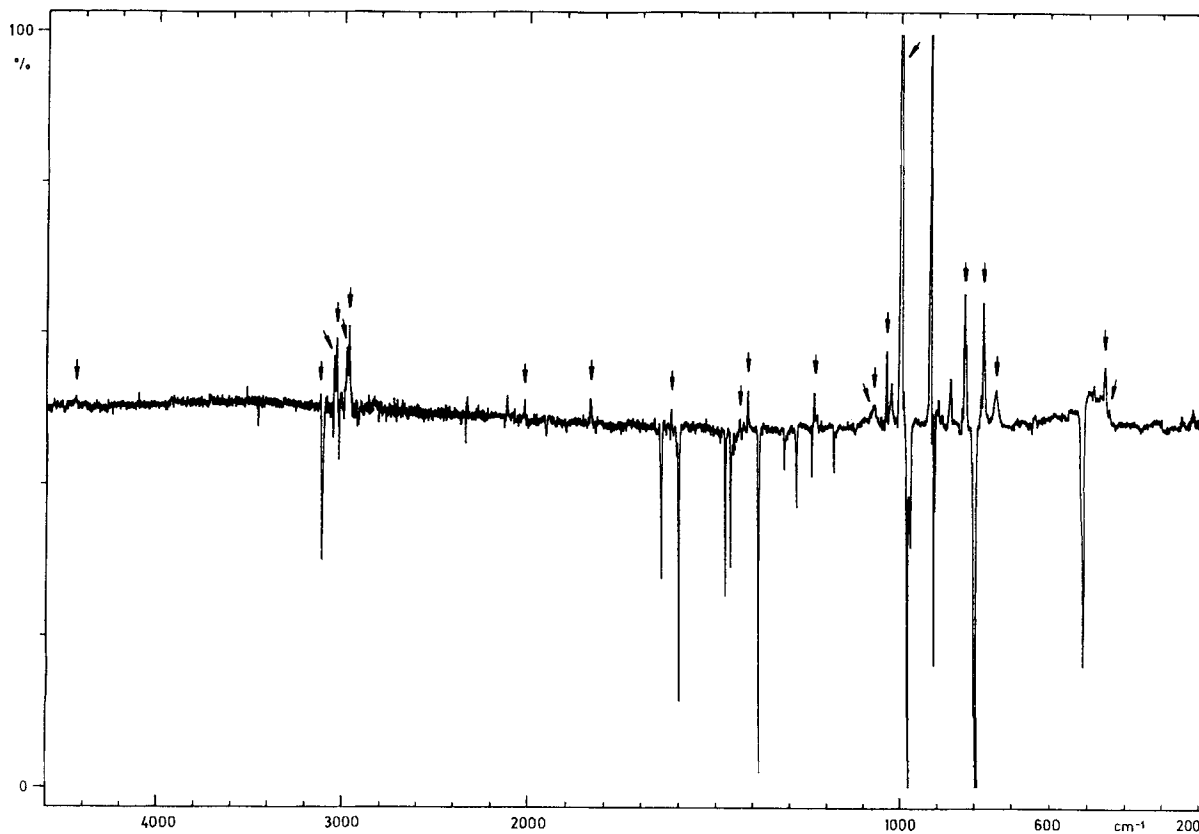
Figure 2. Difference spectrum, providing evidence for the vibration frequencies of the cyclopropyl radical which is formed on photolysis of the allyl radical (spectrum in Figure 1a − spectrum in Figure 1b)

Table 2. IR bands appearing or increasing in intensity on irradiation of the argon matrix at 410 nm (Figure 1b) and their assignment

ν (cm^{-1})		Assignment[a]	ν (cm^{-1})		Assignment[a]	ν (cm^{-1})		Assignment[a]
4425	vw	c.r.	1440	w	c.r. + h	899	vw	
3118	w	c.r.	1416	w	c.r.	887	vw	
3049	w	c.r.	1308	vw	c.r.?	865	w	
3042	w	c.r.	1237	w	c.r.	827	m	c.r.
3033	w	c.r.	1229	vw	c.r.	824	sh	c.r.
2980	w	c.r.	1085	vw	c.r.	784	w	
2965	w	c.r.	1077	w	c.r.	777	m	c.r.
2861	w		1065	vw		743	w	c.r.
2125	w		1037	m	c.r.	482	vw	c.r.
2030	vw	c.r.	1028	m		452	w	c.r.
1841	w	c.r.	1024	m		442	vw	c.r.
1623	m	c.r.?	997	w	c.r. + h			

[a] c.r., Cyclopropyl radical; h, hexadiene.

Table 3. IR bands appearing or increasing in intensity on warming of the argon matrix to 37 K
(Figure 1c)

ν (cm^{-1})	Assignment[a]	ν (cm^{-1})	Assignment[a]	ν (cm^{-1})	Assignment[a]
3087	s	1170	vw/b	bcp + hex.r.	962	m	hex.r. + bcp
3016	s	cp + bcp	1094	w	bcp	899	w	hex.r.
2125	w	hex.r.	1065	vw	hex.r.	886	w	bcp
1890	w	cp	1045	w	bcp	865	s	cp
1434	w	cp	1028	s	cp	853	w	cp
429	vw	bcp + hex.r.	1024	s	cp	813	w	bcp
1387	w	bcp + hex.r.	1020	sh	bcp	784	s	hex.r.
1258	w	hex.r.	975	w	hex.r.			
1188	vw/b	hex.r.	968	m	hex.r.			

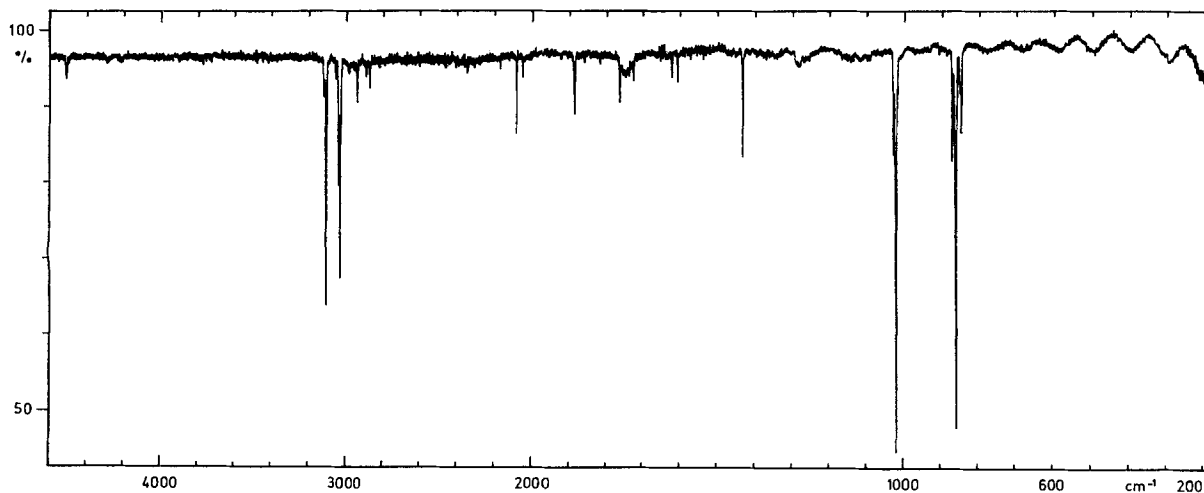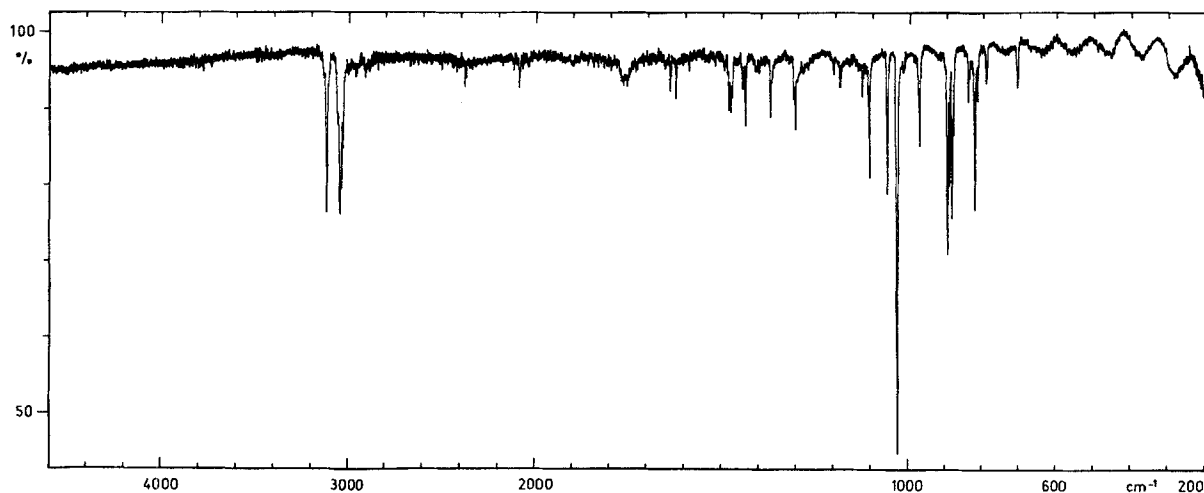[a] cp, Cyclopropane; bcp, bicyclopropyl; hex.r., hexadienyl radical.

Figure 3. IR spectrum of cyclopropane in an argon matrix at 18 K (1·6 μmol cm^{-2} cyclopropane; matrix/host ratio = 1200 : 1)

Figure 4. IR spectrum of bicyclopropyl in an argon matrix at 18 K (0·8 μmol cm^{-2} bicyclopropyl; matrix/host ratio = 3200 : 1)

Table 4. Observed vibration frequencies of cyclopropane trapped in an argon matrix at 18 K[a]

ν (cm^{-1})			ν (cm^{-1})		ν (cm^{-1})		
4496	w		2861	w	1032	w	(−)
3104	w	(−)	2082	w	1025	vs	
3091	s		2048	vw	1020	w	(−)
3041	vw	(−)	1886	w	876	m	(−)
3024	m	(−)	1762	w	865	vs	
3016	s		1726	w	855	w	
2928	w		1435	m	851	m	
2880	vw		1285	w			

[a] The sign (−) indicates that the corresponding band does not decrease appreciably and does not change in position when the matrix is annealed (18 → 28 → 37 → 28K) in the same manner as the matrix containing cyclopropyl radicals.

Table 5. Observed vibration frequencies of bicylopropyl trapped in an argon matrix at 18 K[a]

ν (cm^{-1})			ν (cm^{-1})			ν (cm^{-1})		
3100	w	(−)	1431	w		960	m	
3085	m		1424	w		886	m	
3026	w	(−)	1356	w		880	m	(−)
3015	m		1294	w	(−)	873	w	
3010	m	(sh)	1289	w		869	w	
3000	w	(sh)	1188	vw	(−)	829	m	
2054	w		1170	w		812	w	
1745	w		1111	w		803	w	
1467	w		1093	m		781	w	
1462	w		1046	m		697	w	
1458	w		1018	s				

[a] See Table 4.

our *ab initio* frequency computations. The value 3·9 kcal mol^{-1} compares well with the *ab initio* results of Ellinger *et al.*[20]
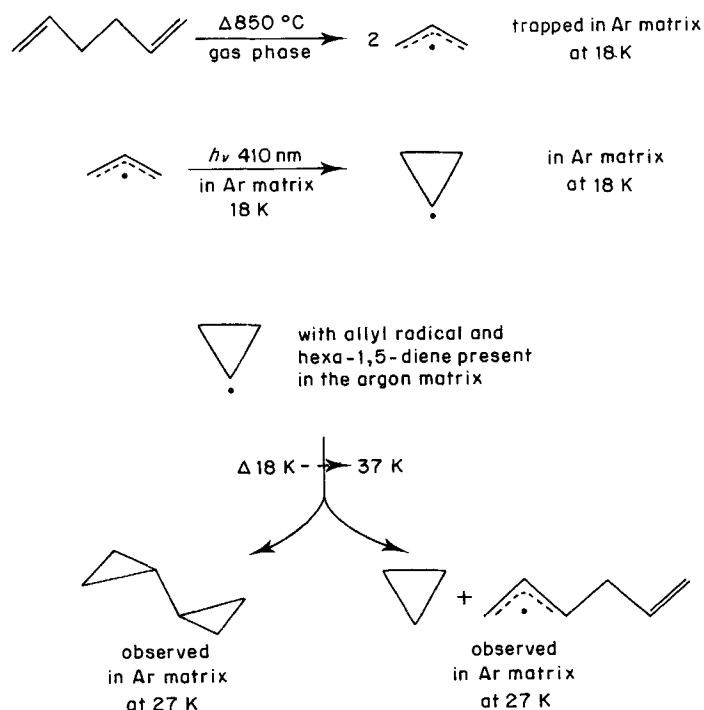
Computation of vibrational frequencies

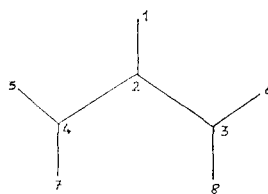The vibrational frequencies of allyl and of cyclopropyl (C_s and C_{2v} symmetry) were computed at the UHF/6-31G* level for UHF/6-31G* optimized geometries. The force constants were determined analytically through second differentiation. The vibrational frequencies obtained are reported in Tables 10 (for allyl) and 11 (for cyclopropyl of symmetry C_s) under the heading 'analytical.' The frequencies resulting from numerically computed force constants are reported under the heading 'numerical.' As can be seen, there is almost no difference between the frequencies obtained by the two methods.
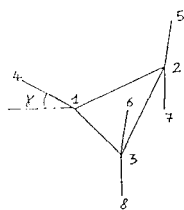

Scheme 1

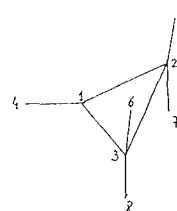Table 6. *Ab initio* optimized geometry for allyl radical C_{2v}[a]

Parameter	6-31G*	6-31G**	D95**	MP2/6-31G*
Bond lengths (Å)				
H_1C_2	1·078	1·079	1·079	1·088
C_2C_3	1·390	1·390	1·396	1·377
C_4H_5	1·074	1·074	1·076	1·082
C_4H_7	1·076	1·076	1·077	1·084
Bond angles (°)				
$C_3C_2C_4$	124·6	124·5	124·5	124·4
$H_5C_4C_2$	121·4	121·4	121·1	121·8
$H_7C_4C_2$	121·2	121·2	121·1	121·0

[a] Numbering of the atoms adopted:

Allyl radical C_{2v}

Table 7. *Ab initio* optimized geometry for cyclopropyl radical with C_s symmetry[a]

Parameter	6-31G*	6-31G**	D95**	MP2/6-31G*
Bond lengths (Å)				
C_1C_2	1·470	1·469	1·477	1·469
C_2C_3	1·517	1·517	1·523	1·526
C_1H_4	1·072	1·072	1·074	1·081
C_2H_5	1·078	1·078	1·078	1·087
C_2H_7	1·078	1·078	1·078	1·087
Bond angles (°)				
γ	41·1	40·8	41·1	41·1
$C_2C_1C_3$	62·2	62·2	62·2	62·6
$C_1C_2H_5$	118·9	118·9	118·7	119·1
$C_1C_2H_7$	118·5	118·5	118·3	118·7
Torsion angles:				
$C_1C_2C_3H_5$	106·5	106·5	106·4	105·3
$C_1C_2C_3H_7$	−107·4	−107·7	−107·8	−108·2

[a] Numbering of the atoms adopted:

Cyclopropyl radical C_s

Table 8. *Ab initio* optimized geometry for cyclopropyl radical with C_{2v} symmetry[a]

Parameter	6-31G*
Bond lengths (Å)	
C_1C_2	1·456
C_2C_3	1·529
H_4C_1	1·066
H_5C_2	1·080
Bond angles (°)	
$C_3C_1C_2$	63·38
$H_5C_2C_1$	119·35
Torsion angles:	
$C_1C_2C_3H_5$	106·32

[a] Numbering of the atoms adopted:

Cyclopropyl radical C_{2v}

In Table 10, the vibrational frequencies of the allyl radical calculated by Takada and Dupuis[13] (multi-configuration Hartree–Fock MHCF) and by us are compared with the experimental frequencies, the deviations between the computed and experimental values being reported as percentages. As can be seen, the 6-31G* basis set reproduces the experimental data reasonably well, the mean deviation being 9·3% with the *ab initio* computed frequency being greater than the observed value; the greatest discrepancy is observed for the CH_2 rocking model ρ_aCH_2 (experimental 810 cm^{-1}; computed 1005–1006 cm^{-1}; deviation 24·1%).

It is well known that *ab intio* computed frequencies are always ca 10% greater than the corresponding normal frequencies obtained from gas-phase measurements on model substances. A scaling procedure is generally adopted to bring the computed frequency in accord with experience. A uniform scaling factor σ (*ab initio*), which is defined as the average ratio of assigned experimental frequencies $\nu_i(\exp)$ to the corresponding *ab initio* computed frequencies $\nu_i(ab\ initio)$, the averaging being performed over the normal modes of many model compounds in the gas phase, was used. For the level of theory employed here (HF/6-31 G*), such scaling factors based on the ratios $\nu_i(\exp)/\nu_i(HF/6-31\ G*)$ for 165 frequencies in molecules constructed from only first-row elements have been deduced from the work of Hout *et al.*[21] by DeFrees and McLean[22]: $\sigma(UHF/6-31\ G*) = 0·89$.

Table 9. Total *ab initio* energy (E_{tot}) of allyl and cyclopropyl radicals (C_s and C_{2v}) as computed with GAUSSIAN82 program using different basis sets

Radical	Symmetry	State	E_{UHF}(a.u.)			
			6-31G*	6-31G**	D95**	MP2/6-31G*
Allyl	C_{2v}	$^2A_2$	$-116\cdot46811$	$-116\cdot47699$	$-116\cdot49362$	$-116\cdot82429$
Cyclopropyl	C_s	$^2A'$	-116.41554	-116.42438	-116.43993	-116.79204
Cyclopropyl	C_{2v}	$^2B_1$	-116.4093	—	—	—

Table 10. Assignment of the identified IR absorptions of allyl radical (Figure 1a, Table 1) to its normal mode, taking advantage of *ab initio* computed frequencies

Vibrational mode	Symmetry	Experimental frequency (cm^{-1})	*Ab initio* HCHF[13] (cm^{-1})	Deviation (%)	*ab intio* UHF/6-31G*					
					Analytical (cm^{-1})	Deviation (%)	Numerical (cm^{-1})	Deviation (%)	Scaled (cm^{-1})	Deviation (%)
ν_aCH_2	A_1	3109	3413	9·8	3422	10·1	3421	10·0	3045	$-2\cdot2$
ν_aCH_2	B_2	3109	3407	9·6	3418	9·9	3417	9·9	3041	$-2\cdot2$
νCH	A_1	3051	3327	9·0	3336	9·3	3316	8·7	2951	$-3\cdot3$
ν_sCH_2	A_1	3019	3318	9·9	3325	10·1	3334	10·4	2967	$-1\cdot7$
ν_sCH_2	B_2	3019	3314	9·8	3324	10·1	3325	10·1	2959	$-2\cdot0$
δ_sCH_2	A_1	1478	1661	12·4	1647	11·4	1647	11·4	1466	$-0\cdot8$
δ_sCH_2	B_2	1464	1632	11·5	1637	11·8	1638	11·9	1458	$-0\cdot4$
δCH	B_2	1389	1556	12·0	1537	10·6	1537	10·6	1368	$-1\cdot5$
ν_aCC	B_2	1284	1204	$-6\cdot2$	1251	$-2\cdot6$	1254	$-2\cdot3$	1116	$-13\cdot1$
ρCH_2	A_1	1242	1370	10·3	1341	7·9	1343	8·1	1195	$-3\cdot8$
ν_sCC	A_1	1183	1093	$-8\cdot2$	1075	$-9\cdot1$	1077	$-8\cdot9$	958	$-19\cdot0$
γCH	B_1	984	1051	10·9	1035	5·2	1035	5·2	921	$-6\cdot4$
ρ_aCH_2	B_2	810	1040	28·4	1005	24·1	1006	24·2	895	10·5
ω_sCH_2	B_1	802	786	$-2\cdot0$	799	$-0\cdot4$	799	$-0\cdot4$	711	$-11\cdot3$
ω_aCH_2	A_2	i.a.[a]	761	—	780	—	780	—	694	—
τCH_2	A_2	i.a.[a]	596	—	572	—	572	—	509	—
τCH_2	B_1	511	562	10·0	547	7·0	547	7·0	487	$-4\cdot7$
δCCC	A_1	n.o.[b]	476	—	451	—	452	—	402	—
Mean deviation (%)				10·7		9·3		9·3		5·5

[a] Inactive in IR.
[b] Not observed.

Application of this scaling factor to the 'numerically' computed frequencies gives the data reported under the headings 'scaled.' This arbitrary scaling procedure improves the computed data, as can be seen from Table 10: the scaled UHF/6-31G* frequencies are now only few percent smaller than the observed values. A mode-by-mode scaling procedure in fact leads to even better results; such a procedure, applied to more elaborate *ab initio* computed frequencies, will be discussed elsewhere.[23]

In the case of the cyclopropyl radical with C_s symmetry, the mean average deviation for our computed frequencies (12·4%) and of those of Dupuis and Pacansky[9] is greater than in the case of allyl. Comparing our results with those of Dupuis and Pacansky,[9] we realised that the latter workers erroneously assigned the

frequency computed at 870 cm^{-1} to the CH$_2$ symmetrical twist mode (A') and the frequency computed at 1241 cm^{-1} to the CH$_2$ symmetrical rocking mode (A'). In fact, the assignment of these two computed frequencies has to be reversed as we have found in our computation and by reproducing the computation of Dupuis and Pacansky. The agreement between these computed frequencies and the frequencies observed at 1037 and 743 cm^{-1} is then better (these frequencies are given in italics in Table 11). Here again the scaling procedure adopted improves the computed frequencies but a mode-by-mode scaling method leads to an even better improvement.[23]

The *ab initio* computed frequencies for the cyclopropyl π-radical (C_{2v} symmetry) are listed in Table 12. Comparison of these computed frequencies

Table 11. Assignment of the identified IR absorptions of cylopropyl radical (C_s) (Figure 1b, Table 2) to its normal mode, taking advantage of *ab initio* computed frequencies

| Vibrational mode | Symmetry | Experimental frequency (cm^{-1}) | *Ab initio*[9] (cm^{-1}) | Deviation (%) | UHF/6-31G* | | | | | |
					Analytical (cm^{-1})	Deviation (%)	Numerical (cm^{-1})	Deviation (%)	Scaled (cm^{-1})	Deviation (%)
νCH	A'	3118	3418	9·6	3406	9·2	3407	9·3	3032	−2·8
ν_aCH$_2$	A'	3049 / 3042	3373	10·8	3367	10.4	3369	10·6	2998	−1·5
ν_aCH$_2$	A''	3033	3358	10·7	3354	10·6	3355	10·6	2986	−1·5
ν_sCH$_2$	A'	2980	3293	10·5	3291	10·4	3292	10·5	2930	−1·7
ν_sCH$_2$	A''	2965	3286	10·8	3285	10·8	3286	10·8	2925	−1·4
δCH$_2$	A'	1440	1646	14·2	1645	14·2	1645	14·2	1464	−1·7
δCH$_2$	A''	1416	1623	14·6	1604	13·3	1604	13·3	1428	0·8
δ_sCCC	A'	1237	1314	6·2	1339	8·2	1339	8·2	1192	−3·7
τ_aCH$_2$	A''	1229	1301	5·8	1287	4·7	1287	4·7	1145	−7·3
γCH	A''	1085	1208	11·3	1190	9·7	1196	10·2	1064	−1·9
τ_sCH$_2$	A'	1077	*870*	−23·8	1230	14·2	1246	15·7	1109	−3·0
ω_aCH$_2$	A''	1037	1268	22·2	1209	16·6	1209	16·6	1076	−3·8
ω_sCH$_2$	A'	997	1204	20·8	1169	17·3	1169	17·3	1040	4·3
ν_aCC	A''	n.o.[a]	995	—	1007	—	1008	—	897	—
ν_sCC	A'	827 / 824	916	11·1	930	12·5	931	12·8	828	0·4
ρCH$_2$ + γCH	A''	777	893	14·9	847	9·0	847	9·0	754	−3·1
ρCH$_2$ + δCH	A'	743	*1241*	67·0	855	13·1	855	13·1	761	2·4
δCH	A'	n.o.[a]	713	—	704	—	705	—	627	—
Mean deviation (%)				16·5		11·5		11·5		−2·5

[a] Not observed.

Table 12. Computed ('numerical') vibrational frequencies (in cm^{-1}) for the cyclopropyl radical (C_{2v}) normal modes

| Vibrational mode | Symmetry | UHF/6-31G* | |
		Numerical (cm^{-1})	Scaled (cm^{-1})
νCH	A_1	3478	3095
ν_aCH$_2$	B_1	3340	2973
ν_aCH$_2$	A_2[a]	3325	2959
ν_sCH$_2$	A_1	3267	2808
ν_sCH$_2$	B_2	3262	2803
CH$_2$ bend + CH$_2$ wag	A_1	1645	1464
CH$_2$ bend + CH$_2$ wag	B_2	1608	1431
ν_sCCC + CH$_2$ wag	A_1	1348	1200
ρCH$_2$	A_2[a]	1270	1130
ωCH	B_2	1219	1085
ω_sCH$_2$	A_1	1190	1059
αCC asym. stretch	B_2	1160	1032
τ_sCH$_2$	B_1	1129	1005
αCH wag	B_2	948	844
τ_aCH$_2$	A_2[a]	933	830
βCC sym. stretch	A_1	918	817
ρCH$_2$	B_1	834	742
αCH bend	B_1	−671im[b]	−597im[b]

[a] Vibration with A_2 symmetry and inactive in IR.
[b] im, Imaginary frequency.

(14 IR active + 1 imaginary) with the experimental frequencies reported in Table 3 clearly indicates that a concordance between experimental and calculated frequencies could be established. However, of all the computed vibrational frequencies for cyclopropyl with C_{2v} symmetry, the lowest one (677 cm^{-1}) is imaginary. It has B_1 symmetry and corresponds to the out-of-plane motion of the proton at the radical centre. The existence of this imaginary frequency implies that the π-radical should be the transition-state structure for the inversion at the σ radical centre of the cyclopropyl radical.

REFERENCES

1. G. Greig and J. C. Thynne, *Trans. Faraday Soc.* **63**, 1369–1374 (1967).
2. G. Greig and J. C. Thynne, *Trans. Faraday Soc.* **62**, 3338–3344 (1966).
3. D. Schneider, PhD Thesis, Munich (1977).
4. S. Sustmann, Ch. Rüchardt, A. Bieberbach and G. Boche, *Tetrahedron Lett.* 4759–4764 (1972); S. Sustmann and Ch. Rüchardt, *Tetrahedron Lett.* 4765–4770 (1972).
5. H. M. Walborsky, *Tetrahedron* **37**, 1625–1651 (1981).
6. H. C. Longuet-Higgins and E. W. Abrahamson, *J. Am. Chem. Soc.* **87**, 2045–2046 (1965).
7. G Szeimies and G. Boche, *Angew. Chem., Int. Ed. Engl.* **10**, 911–912 (1971).

8. R. W. Fessenden and R. H. Schuler, *J. Chem. Phys.* **39**, 2147–2195 (1963).
9. M. J. Dupuis and J. Pacansky, *J. Chem. Phys.* **76**, 2511–2515 (1982).
10. J. Dyke, A. Ellis, N. Jonathan, A. Morris, *J. Chem. Soc., Faraday Trans. 2* **81**, 1573–1586 (1985).
11. K. Holtzhauer, PhD Thesis, ETH, Zurich (1987); K. Holtzhauer and J. F. M. Oth, to be published.
12. J. F. M. Oth, to be published.
13. T. Takada and M. J. Dupuis, *J. Am. Chem. Soc.* **105**, 1713–1716 (1983).
14. C. Cometta-Morini, J. F. M. Oth and T.-K. Ha, to be published.
15. J. S. Binkley, M. J. Frisch, D. J. DeFrees, K. Ragavachari, R. A. Whiteside, H. B. Schlegel, E. M. Fluder and J. A. Pople, *GAUSSIAN82*, Carnegie-Mellon University, Pittsburgh, PA (1983).
16. P. C. Hariharan and J. A. Pople, *Theor. Chim. Acta* **28**, 213–222 (1973).
17. M. M. Francl, W. J. Pietro, W. J. Hehre, J. S. Binkley, M. S. Gordon, D. J. DeFrees and J. A. Pople, *J. Chem. Phys.* **77**, 3654–3665 (1982).
18. T. H. Dunning, Jr and P. J. Hay, *Modern Theoretical Chemistry*, vol. 2. Plenum Press, New York (1977).
19. J. A. Pople, J. S. Binkley and R. Seeger, *Int. J. Quantum Chem. Symp.* **10**, 1–20 (1976).
20. Y. Ellinger, R. Subra, B. Levy, P. Millie and G. Berthier, *J. Chem. Phys.* **62**, 10–29 (1975).
21. R. F. Hout, Jr, B. A. Levi and W. J. Hehre, *J. Comput. Chem.* **3**, 234 (1982).
22. D. J. DeFrees and A. D. McLean, *J. Chem. Phys.* **82**, 333 (1985).
23. C. Cometta-Morini, T.-K. Ha and J. F. M. Oth., *J. Mol. Struct. Theochem.* **188**, 79–94 (1989).